Ocean Engineering 361 (2026) 126168

Contents lists available at ScienceDirect

Ocean Engineering

journal homepage: www.elsevier.com/locate/oceaneng

Research paper

A robust COLREG Meta-Classification system for autonomous ships in two-vessel encounter scenarios

Nicola Sabatino *, Raphael Zaccone

Marine, Electrical, Electronics and Telecommunication Engineering and Naval Architecture Department (DITEN), Polytechnic School, University of Genoa, Via Montallegro 1, Genoa, 16145, Italy

ARTICLE INFO

Keywords:
COLREG
Collision avoidance
Autonomous navigation
MASS
Autonomous ship

ABSTRACT

The advent of Maritime Autonomous Surface Ships raises many concerns about the safety of navigation, especially concerning how COLREG-compliant collision avoidance activities should be performed. To address these issues, autonomous navigation systems make use of COLREG Classification systems that detect the rules that apply to a given scenario, and proper algorithms that plan and execute evasive manoeuvres. In the literature, there is a third element that determines when the COLREG Classification system should be triggered and how its output should be handled by the collision avoidance algorithm. This paper proposes the term Meta-Classification system to indicate this third element. The approach to Meta-Classification that makes use only of the current features of an encounter scenario is named by this paper Static COLREG Meta-Classification. Recent works in the literature have identified the issue of Classification Instability in these approach. To solve the issue of Classification Instability this paper proposes a novel approach to Meta-Classification named Dynamic COLREG Meta-Classification. This approach introduces a memory effect which increases the robustness of the classification process in two-vessel encounter scenarios. Static COLREG Meta-Classification and Dynamic COLREG Meta-Classification are compared by means of numerical simulations of encounter scenarios.

1. Introduction

Marine vehicles of increasing autonomy have started to be more and more present in the maritime industry since the 1960s, when the first remotely operated underwater drones were employed in offshore oil & gas extraction activities. The advances in computing and communication technology made in the last decades are allowing autonomous commercial vessels to become a tangible reality, and even the International Maritime Organization (IMO) has begun working on a regulatory framework for the coming advent of Maritime Autonomous Surface Ships (MASSs) (IMO, 2021).

The introduction of MASSs in the maritime industry is expected to increase the efficiency of operations at sea (Alamoush et al., 2024) and to reduce their risk by removing human errors, which, still nowadays, represent the leading cause of accidents at sea (EMSA, 2024). For all these reasons, the development of MASSs is attracting considerable interest from both academia and industry. However, there are still many challenges to solve before MASSs can be fully operational. One of the most pressing challenges is the safety of navigation: the lack of seafarers on board of MASSs is expected for those vessels reaching a level of autonomy of 3 or 4 (IMO, 2021) and this raises the problem of how to make a MASS comply with current regulations regarding the safe conduct of a vessel. To address this pressing issue, the topic of COLREG-compliant marine Collision Avoidance (CA) has gained significant attention in the scientific literature in recent years.

The process of COLREG-compliant CA for MASS requires two elements: a COLREG Classification (CC) system capable of recognising the rules the MASS must comply with, and a CA algorithm capable of making the MASS deviate from the preplanned route to avoid collisions while complying with the requirements of the rules recognised.

The CA algorithms found in the current literature are, for the most part, derived from collision-free planning algorithms from robotics (Zaccone et al., 2026; Fruzzetti et al., 2026). The first classes of algorithms of this kind are Artificial Potential Field (APF) and Velocity Obstacle (VO). Examples of APF-based algorithms are presented by Wang et al. (2020) and Lyu and Yin (2017), while different VO algorithms are discussed by Huang et al. (2018). More recently, optimal planning algorithms have been proposed, including heuristics such as Ant Colony Optimisation (Lazarowska, 2015), or Particle Swarm Optimization (Kang et al., 2018), Rapidly-Exploring Random Trees (Zaccone and Martelli, 2020; Enevoldsen et al., 2021), grid-based search approaches such as Dijkstra's algorithm (Singh et al., 2017), A* (Seo et al., 2023), Dynamic Programming (Zaccone, 2024). Huang et al. (2020) presents a

* Corresponding author.
E-mail addresses: nicola.sabatino@edu.unige.it (N. Sabatino), raphael.zaccone@unige.it (R. Zaccone).

https://doi.org/10.1016/j.oceaneng.2026.126168
Received 12 December 2025; Received in revised form 28 April 2026; Accepted 19 May 2026
Available online 25 May 2026

comprehensive review of marine CA algorithms. The CC systems found in the literature are, for the most part, based on geometric considerations derived from interpretations of certain COLREGs. A detailed review of state-of-the-art CC systems is presented in Section 2.

The way CC systems are usually implemented make them unable to recognise whether or not it is necessary to classify a certain encounter scenario. Therefore, they cannot be put in direct connection with CA algorithms or they would require unnecessary evasive actions. A third element is then required to determine when the CC system should be used and how its output should be handled by the CA algorithm. This element is referred to as Meta-Classification system in this paper.

Most of the works from literature propose Meta-Classification procedures based on triggering the CC system only when an unacceptable risk of collision is detected. Examples can be found in Zaccone et al. (2019), Cho et al. (2022) and Eriksen et al. (2020). This naive approach is called Static COLREG Meta-Classification (SCMC), as it makes use only of the current features of the encounter scenarios.

However, compared with the way human seafarers handle CA activities at sea, SCMC exhibits a major difference: the lack of memory of the previous states of the encounter scenario. A human seafarer is aware whether a certain situation is the outcome of an ongoing evasive manoeuvre or whether it is a new situation yet to be classified. An SCMC, by its very nature, cannot be aware of that and would continuously reclassify the encounter situation as long as the risk of collision persists. This phenomenon is referred to in this paper as Classification Instability and, as the next sections of this paper will show, it may decrease the performance of a CA system.

To overcome the issue of Classification Instability this paper proposes a novel Meta-Classification technique named Dynamic COLREG Meta-Classification (DCMC), which introduces a rule that determines when it is necessary to reclassify a given encounter scenario. Such rule is referred to in this paper as the Past And Clear Condition (PACC).

The DCMC introduced in this paper is shown to not only solve the issue of Classification Instability, which could be solved by a CA planner or by a CA controller designed to handle it, but makes the output of CC systems more reliable, thus allowing their use for more complex decision-making tasks.

With respect to the current literature this paper offers the following novelties:

- A formulation for the PACC that adapts to each situation;
- An extensive numerical simulation campaign that highlights the issue of Classification Instability and provides insights on the performance of DCMC compared to SCMC.

The remainder of this paper is organised as follows. Section 2 features a literature review of CC systems. Section 3 discusses the issue of Classification Instability. Section 4 introduces a mathematical formulation of the CA problem for MASSs. Section 5 describes DCMC in detail. Section 6 describes the simulations carried out to compare the performance of SCMC and DCMC, and Section 7 presents and discusses the results of such simulations. Finally, Section 8 presents the conclusions of this work and highlights weak points that future works should address.

2. Related works

CC systems are the elements of a marine autonomous navigation system which identify the rules that apply to a given encounter scenario. However, given the vastness and complexity of COLREGs, the literature on CC systems focuses on recognising Rules 13 to 17, which describe overtaking, head-on, and crossing situations, as well as give-way and stand-on behaviours. For this reason a CC system can be considered as a function taking as input the current position, heading, and velocity of the own ship and the target ship and returning a triple (S, B_{OS}, B_{TS}), where S is a situation, B_{OS} is the behaviour required by the own ship, and B_{TS} is the behaviour required by the target ship. In this paper, the terms HO, CR, and OT are used to indicate the head-on, crossing, and overtaking situations respectively, and the terms GW and SO are used to indicate the give-way and stand-on behaviours, respectively.

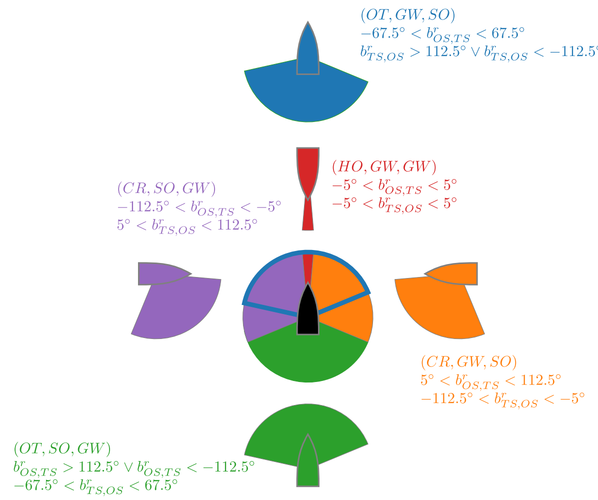

Fig. 1. Bearing-based static classification.

An early attempt at CC can be found in Hasegawa (1987). This work proposes a rule-based controller for automatic collision avoidance which integrates CC reasoning. The main CC methodologies adopted in the current literature are the bearing-based approach and the course-based approach. The bearing-based approach uses the relative bearing of the target ship from the own ship's point of view $b^r_{OS,TS}$ to determine the type of encounter situation. The value of $b^r_{OS,TS}$ is calculated via Eq. (1):

$$b^r_{OS,TS} = \text{sign}\left(\left(\mathbf{v}^n_{OS} \wedge \mathbf{r}_{TS,OS}\right) \cdot \hat{\mathbf{k}}\right) \cos^{-1}\left(\frac{\mathbf{v}^n_{OS} \cdot \mathbf{r}_{TS,OS}}{\left\|\mathbf{v}^n_{OS}\right\| \left\|\mathbf{r}_{TS,OS}\right\|}\right) \tag{1}$$

where:

$$\mathbf{r}_{TS,OS} = (\mathbf{p}_{TS} - \mathbf{p}_{OS}) \tag{2}$$

and $\mathbf{v}^n_{OS}$ and $\mathbf{v}^n_{TS}$ are the velocity vectors of the own ship and target ship, respectively, expressed in the reference frame $\{n\}$, and $\mathbf{p}_{OS}$ and $\mathbf{p}_{TS}$ are the position vectors of the own ship and target ship, respectively. The type of situation and behaviour are determined according to Fig. 1. Bearing-based CC systems have been successfully applied in various scientific papers. Wang et al. (2023) uses it as part of an algorithm based on deep reinforcement learning. Cho et al. (2022) adopts a slightly modified version of the bearing-based approach to guide a probabilistic velocity obstacle-based CA algorithm. Eriksen et al. (2020) employs a bearing-based CC system originally developed by Tam and Bucknall (2010) in a model predictive control-based CA algorithm.

The other main CC methodology is the course-based approach, which relies on the value of the relative course angle between the own ship and the target ship $\Delta\psi_{OS,TS}$. The value of $\Delta\psi_{OS,TS}$ is calculated with Eq. (3):

$$\Delta\psi_{OS,TS} = \text{sign}\left(\left(\mathbf{v}^n_{OS} \wedge \mathbf{v}^n_{TS}\right) \cdot \hat{\mathbf{k}}\right) \cos^{-1}\left(\frac{\mathbf{v}^n_{OS} \cdot \mathbf{v}^n_{TS}}{\left\|\mathbf{v}^n_{OS}\right\| \left\|\mathbf{v}^n_{TS}\right\|}\right) \tag{3}$$

The situation and behaviours are determined according to Table 1. The course-based approach has been proven effective in Zaccone (2024), where it is used to generate the constraint of a dynamic programming problem to plan evasive manoeuvres. Martelli et al. (2024) uses the course-based approach for collision detection and classification.

Table 1
Course-based static classification.

Relative course	Situation
$-175° \le \Delta\psi_{OS,TS} \le 175°$	(HO, GW, GW)
$-175° \le \Delta\psi_{OS,TS} \le -67.5°$	(CR, SO, GW)
$67.5° \le \Delta\psi_{OS,TS} \le 175°$	(CR, GW, SO)
$\lvert\Delta\psi_{OS,TS}\rvert \le 67.5°$	(OT, GW, SO) or (OT, SO, GW)

Besides these main methods, in recent years machine learning-based approaches have also emerged. Examples can be found in Namgung and Kim (2021), which utilised fuzzy logic-based CC system, and in Meyer et al. (2020), which employed deep reinforcement learning.

Despite their simplicity and effectiveness, bearing-based and course-based methods do not embed any procedure to assess whether or not two vessels are on colliding routes. Therefore, if used alone, these CC methodologies could mistakenly classify encounter situations where there is no actual risk of collision. To avoid these problems, as already stated in Section 1, CC systems must be handled by Meta-Classification systems. Many works in the literature employ a similar approach for Meta-Classification: a scenario is classified only when an unacceptable risk of collision is detected. Such a Meta-Classification system is referred to in this paper as SCMC. In Zaccone et al. (2019) the CC system is triggered when the distance between the own ship and the target ship is less than a given threshold. In Cho et al. (2022) and in Eriksen et al. (2020) risk of collision is deemed to exist between two vessels using the CPA-TCPA method, presented later in this paper.

The element of an SCMC system responsible for detecting the presence of a risk of collision is referred to as Collision Risk Assessment (CRA) methodology. CRA methodologies are widely studied in the field of marine autonomous navigation. There are three main approaches to CRA: the Collision Risk Index (CRI), the Ship Domain (SD) and the CPA-TCPA method.

The CRI is a metric function that quantifies the risk of collision. There are different methods from literature to calculate it, but generally it is a function of the position, course, and speed of both the own ship and the target ship, and it ranges between a minimum of 0 and a maximum of 1. CRI-based CRA systems deem a risk of collision to exist if the CRI exceeds a threshold limit. Huang et al. (2020) presented a comprehensive review of different method for the calculation of the CRI.

The Ship Domain (SD) is a virtual region of space surrounding a vessel. SD-based CRA systems deem a collision risk to exist if the own ship's SD gets violated in some way by the target ship. To determine whether a violation occurs, different approaches can be adopted. In Fujii and Tanaka (1971), the first publication to introduce the concept of SD, the own ship's SD is considered violated when the target ship crosses it. Tam and Bucknall (2010) considered the SD to be violated if the target ship's future trajectory crosses it. In Kijima and Furukawa (2003), the target ship's SD is also taken into account: a collision is deemed to exist if the two vessels' SDs are overlapping. For a review of SD-based CRA systems, one should refer to Huang et al. (2020).

The CPA-TCPA method for CRA is widely adopted by seafarers and is based on the concept of Closest Point of Approach, i.e., the point in space where the distance between two vessels is going to be at its minimum if the vessels keep their current course and speed. Two quantities are relevant for this method: the distance between the two vessels V_1 and V_2 at the Closest Point of Approach, indicated as $CPA_{V_1,V_2}(t)$, and the Time to Closest Point of Approach, i.e., the time interval before the vessels are expected to reach the Closest Point of Approach, indicated as $TCPA_{V_1,V_2}(t)$. $CPA_{V_1,V_2}(t)$ and $TCPA_{V_1,V_2}(t)$ are calculated as described in Eqs. (4) and (5):

$$CPA_{V_1,V_2}(t) = \min_t \left\| \mathbf{p}_{V_1,V_2}(t) + t\mathbf{v}^n_{V_1,V_1}(t) \right\| \tag{4}$$

$$TCPA_{V_1,V_2}(t) = \operatorname*{argmin}_t \left\| \mathbf{p}_{V_1,V_2}(t) + t\mathbf{v}^n_{V_1,V_1}(t) \right\| \tag{5}$$

where $\mathbf{p}_{V_1,V_2}(t)$ and $\mathbf{v}^n_{V_1,V_1}(t)$ are the relative position at time t and relative velocity expressed in the $\{n\}$ reference frame between the two vessels, respectively. According to the CPA-TCPA method, risk of collision is deemed to exist when $CPA_{V_1,V_2}(t)$ and $TCPA_{V_1,V_2}(t)$ are below certain threshold values CPA_{alert} and $TCPA_{alert}$ which are usually determined according to good seamanship practice.

SCMC systems have been proven effective in many works. However, since their output is based only on the current features of the encounter scenario, they are prone to the phenomenon of Classification Instability, properly described in Section 5. Gleeson et al. (2024) addresses Classification Instability in the context of COLREG compliance evaluation by assigning different priority levels to COLREG situations and using a condition on the distance between vessels to decide whether to reclassify a scenario.

3. Description of classification instability

This section aims to clarify what Classification Instability is and how it could affect the process of COLREG-compliant CA for MASS.

The current literature on COLREG-compliant CA is highly focused on "solving" encounter scenarios between MASSs, and, most of the time, CA systems are validated in simulations where planning and executing an evasive manoeuvre is the only mission objective. However, in reality, CA is only one of the many tasks a MASS must carry out during its operation to achieve its mission objective. When SCMC is applied in a realistic context where multiple conflicting tasks need to be performed, its drawbacks start to emerge.

Fig. 2 shows schematically how SCMC may fail in guiding a MASS through an evasive manoeuvre. In the picture, the blue MASS and the red MASS are sailing along the same route, but in opposite directions. At t_1, their CRA systems detect a risk of collision. Therefore, according to the SCMC methodology, their CC systems are triggered and correctly classify the scenario as a head-on situation. As a consequence, both MASSs start to turn starboard. At t_2, due to the evasive manoeuvres, the two MASSs are on parallel routes, thus their CRA methodologies do not recognise a risk of collision, therefore, according to the SCMC methodology, their CC systems are not triggered. This causes the MASSs to believe that it is not necessary to execute an evasive manoeuvre, causing them to revert to their original path following task, eventually causing a collision at t_3.

This phenomenon of changing the classification output in the middle of an evasive manoeuvre is what this paper refers to as Classification Instability. Although theoretically, the scenario described in Fig. 2 shows how Classification Instability can bring SCMC to failure. At the core of Classification Instability there is lack of a memory of the previous states of the encounter scenario: a human seafarer would recognise the situation at t_2 as originating from an evasive manoeuvre and would continue the manoeuvre until past-and-clear from the other vessel; an SCMC is, by design, incapable of such behaviour.

To tackle the issue of Classification Instability, this paper introduces the DCMC methodology, which would implement a behaviour closer to human reasoning by introducing a memory effect in the classification process.

4. Marine collision avoidance framework

Before proceeding with the description of DCMC, it is necessary to define the kinematics of vessels and provide a mathematical formulation of the CA problem.

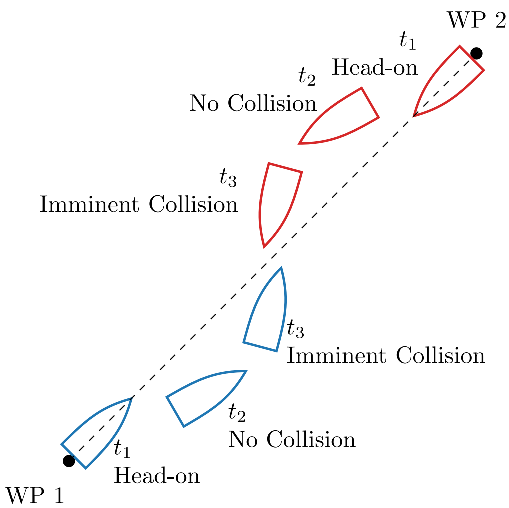

Fig. 2. Schematic representation of the instability mechanism of static COLREG Classification.

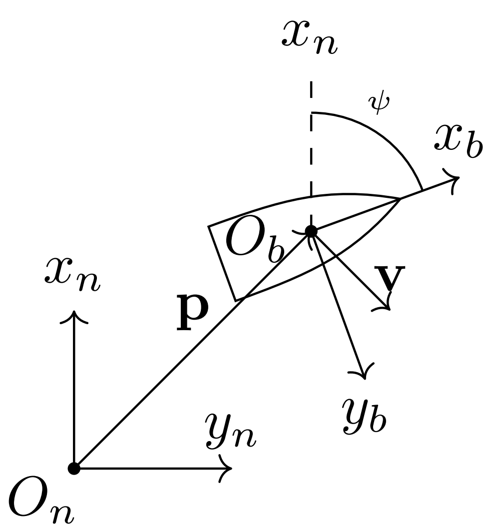

Fig. 3. Vessel kinematics.

4.1. Vessel kinematics

The vessel kinematics description employed in this paper is based on Fossen (2011). Two reference frames are defined: the Earth-fixed reference frame $\{n\}$, and the body-fixed reference frame $\{b\}$. The reference frame $\{n\}$ is centred on an arbitrary point $\mathcal{O}_n$ on Earth, and its axes x_n and y_n are positive moving from South to North and from West to East, respectively. The reference frame $\{b\}$ is centred on the vessel midship point, and its axes x_b and y_b are positive moving from stern to bow and from port side to starboard, respectively.

The position of the vessel on the surface of the Earth is expressed with respect to $\{n\}$ and is denoted by the vector $\mathbf{p}$, which elements are x and y and represent the position on the axes x_n and y_n respectively, while its heading angle, i.e., angle between x_n and x_b, is indicated by ψ. The velocity of a vessel is expressed with respect to $\{b\}$ and is denoted by the vector $\mathbf{v}$, whose elements are u and v, and represent the speeds along axes x_b and y_b respectively. The velocities u and v are referred to as surge and sway speeds, respectively. The rate of change of ψ is denoted by r and is referred to as yaw rate. All the kinematics quantities discussed are shown in Fig. 3.

Finally, the vectors $\boldsymbol{\eta}$ and $\boldsymbol{\nu}$ are defined as the concatenation of $\mathbf{p}$ with ψ and $\mathbf{v}$ with r, respectively. The vectors $\boldsymbol{\eta}$ and $\boldsymbol{\nu}$ are not independent of each other and their relation is shown in Eq. (6):

$$\dot{\boldsymbol{\eta}} = \mathbf{R}(\psi)\boldsymbol{\nu} \tag{6}$$

where:

$$\mathbf{R}(\psi) = \begin{pmatrix} \cos(\psi) & -\sin(\psi) & 0 \\ \sin(\psi) & \cos(\psi) & 0 \\ 0 & 0 & 1 \end{pmatrix} \tag{7}$$

The concatenation of $\boldsymbol{\nu}$ and $\boldsymbol{\eta}$ is the state vector of the vessel and is indicated as $\mathbf{x}$.

4.2. Two-vessel collision avoidance problem formulation

According to the notation introduced in Section 4.1 the dynamics of a vessel can be described by Eq. (8):

$$\begin{cases} \dot{\boldsymbol{\eta}}(t) = \mathbf{R}(\psi)\boldsymbol{\nu}(t) \\ \dot{\boldsymbol{\nu}}(t) = f(\boldsymbol{\nu}(t), \mathbf{u}(t)) \end{cases} \tag{8}$$

where $f(\cdot)$ is a system function and $\mathbf{u}(t)$ is a vector of input commands.

COLREG-compliant CA in two-vessel scenarios can be defined according to Definition 1:

Definition 1. COLREG-compliant CA is the process of steering a vessel away from the planned route so as to avoid collision with other vessels while complying with the requirements of COLREG.

Consistently with Definition 1 and Eq. (8) it is possible to define the COLREG-compliant CA problem stated in Definition 2:

Definition 2. Given a target ship on a collision route with the own ship, the COLREG-compliant CA problem consists of finding a control strategy $\mathbf{u}(t)$ that would steer the own ship away from the planned route so that it avoids collision with the target ship while complying with the requirements of COLREG.

Therefore, consistent with Definition 2, a mathematical formulation of the COLREG-compliant CA problem requires formalising what avoiding a collision means and the requirements of COLREG. Avoiding a collision can be easily formalised with a condition on the relative distance between the own ship and the target ship. This condition is represented in Eq. (9):

$$\forall t \in [t_d, t_e].\ d_{OS,TS}(t) \geq d_{safety} \tag{9}$$

where t_d is the detection time, i.e., the time at which collision risk is detected for the first time, t_e is the time at which the evasive manoeuvre ends, i.e., the time at which the vessels are past-and-clear, d_{safety} is the minimum distance that must be kept from the target ship to ensure the safety of the own ship, and $d_{OS,TS}(t)$ is the euclidean distance between the own and target ships at time t, defined as in Eq. (10):

$$d_{OS,TS}(t) = \left\|\mathbf{p}_{OS}(t) - \mathbf{p}_{TS}(t)\right\| \tag{10}$$

where $\mathbf{p}_{OS}(t)$ and $\mathbf{p}_{TS}(t)$ are the positions of the own ship and the target ship.

The formalisation of the requirements from COLREG is a much more challenging task, and it remains an open problem in the field of marine autonomous navigation. However, most works from the literature focus on the requirements of rules 8 and 13 to 17, as these are the rules that actively affect how vessels are required to conduct evasive manoeuvres. Since it is beyond the scope of this paper to provide a formalisation of all the requirements from COLREG, only those from rules 8 and 13 to 17 are considered.

Rules 13 to 17 describe the situations involving head-on, crossing, and overtaking, and define the obligations associated with the give-way and stand-on behaviours. In the overtaking situation, the give-way vessel is required to keep out of the way of the stand-on vessel; thus, when the own ship is the give-way vessel in an overtaking situation, the requirement from Eq. (9) is enough. Instead, in the head-on and crossing situations, the give-way vessel has additional requirements: in the head-on situation, it is required to avoid the collision by turning to starboard, and in the crossing situation, it is required to avoid the collision by passing astern of the target ship. The requirement for the head-on situation can be ensured constraining the relative bearing of the target ship with respect to the own ship to be negative. This condition is shown in Eq. (11):

$$\forall t \in [t_d, t_e].\, b^r_{OS,TS}(t) < 0 \tag{11}$$

The requirement for the crossing situation can be ensured constraining the Bow Crossing Range (BCR) of the own ship from the target ship point of view to be negative. The BCR is a quantity originating from seamanship practice which is equal to the signed distance between the two vessels when one vessel crosses the longitudinal symmetry plane of the vessel for which the BCR is calculated. If this crossing happens astern of the vessel for which the BCR is calculated, then the BCR is negative, otherwise, it is positive. The negative BCR condition is shown in Eq. (12):

$$\forall t \in [t_d, t_e].\, BCR_{TS,OS}(t) < 0 \tag{12}$$

$BCR_{TS,OS}(t)$ is calculated as described in Eq. (13):

$$BCR_{V_1,V_2}(t) = x_{V_1,V_2}(t) - y_{V_1,V_2}(t)\frac{V_{x_{V_1,V_2}}}{V_{y_{V_1,V_2}}} \tag{13}$$

where $x_{V_1,V_2}(t)$ and $y_{V_1,V_2}(t)$ are the elements of $\mathbf{p}_{V_1,V_2}(t)$ and $V_{x_{V_1,V_2}}$ and $V_{y_{V_1,V_2}}$ are the elements of $\mathbf{v}^n_{V_1,V_2}$.

Finally, Rule 8 imposes that all actions taken to avoid the collision must be large enough to be readily apparent to other ships. This requirement is formulated in Eqs. (14) and (15):

$$\max\left(\{|\psi(t) - \psi(t_d)| \,:\, \forall t > t_d\}\right) \geq \Delta\psi_{app} \tag{14}$$

$$\begin{aligned}&(\max\left(\{|U(t) - U(t_d)| \,:\, \forall t > t_d\}\right) \geq \Delta U_{app})\\ &\vee (\forall t > t_d.\, U(t) = U(t_d))\end{aligned} \tag{15}$$

where $\Delta\psi_{app}$ is the apparent course change threshold, ΔU_{app} is the apparent speed change threshold, and $U(t)$ is the Speed Over Ground, i.e., the modulus of $\mathbf{v}(t)$. Notice that the constraints in Eq. (14) and (15) could potentially be satisfied by a spike in the values of $\psi(t)$ and $U(t)$, making them ineffective. However, because this paper focuses on MASSs, which are characterised by slow dynamics, this issue can be safely neglected. Any spike in $\psi(t)$ and $U(t)$ originated from a failure in the proprioceptive sensor suite of the vessel is also neglected.

The requirements for the stand-on vessel, regardless of the situation type, are to keep course and speed and are formalised in Eq. (16):

$$\forall t \in [t_d, t_e].\, (\psi(t) = \psi(t_d)) \wedge (U(t) = U(t_d)) \tag{16}$$

Therefore, the COLREG-compliant CA problem can be solved by finding $\mathbf{u}(t)$ such that Eqs. (9), (11), (12) and (14)–(16) are satisfied. This problem, however, may have multiple solutions, which is impractical. Therefore, additional requirements should be imposed to ensure the solution is unique. To tackle this issue, minimising the deviation from the planned route is required. The COLREG-compliant CA problem can then be formulated as the Optimal Control Problem (OCP) in Eq. (17):

$$\begin{aligned}&\underset{\mathbf{u}(t)}{\operatorname{argmin}} \int_{t_d}^{t_e} \left\|\boldsymbol{\eta}_{OS}(t) - \boldsymbol{\eta}_{route}(t)\right\|^2_{\mathbf{P}}\, dt\\ &\quad \text{s.t. C1: } \forall t > t_d.\, d_{OS,TS}(t) \geq d_{safety}\\ &\qquad \text{C2: } (\boldsymbol{\eta}_{OS}(t), \boldsymbol{\nu}_{OS}(t)) \in \mathbb{X}_{COLREG}\\ &\qquad \text{C5: } \mathbf{u}_{max} \leq \mathbf{u}(t) \leq \mathbf{u}_{min}\\ &\qquad \text{C6: } \begin{cases}\dot{\boldsymbol{\eta}}_{OS}(t) = \mathbf{R}(\psi)\boldsymbol{\nu}_{OS}(t)\\ \dot{\boldsymbol{\nu}}_{OS}(t) = f(\boldsymbol{\nu}_{OS}(t), \mathbf{u}(t))\end{cases}\\ &\qquad \text{C7: } \begin{cases}\dot{\boldsymbol{\eta}}_{TS}(t) = \mathbf{R}(\psi)\boldsymbol{\nu}_{TS}(t)\\ \dot{\boldsymbol{\nu}}_{TS}(t) = g(\boldsymbol{\nu}_{TS})\end{cases}\end{aligned} \tag{17}$$

where $\boldsymbol{\eta}_{route}(t)$ is the vector of the expected position and heading according to the planned route, $\mathbf{P}$ is a weighting matrix applied to the norm $\|\cdot\|^2$, $\mathbb{X}_{COLREG}$ is a feasible state set defined by COLREG-compliance constraints, $\mathbf{u}_{max}$ and $\mathbf{u}_{min}$ are the saturation values of the input vector, and $g(\cdot)$ is the system function for the predictive model of the target ship. Notice that the predictive model for the target ship is assumed to be an autonomous system since the input vector of the target ship is unknown. $\mathbb{X}_{COLREG}$ is defined differently depending on the type of situation and behaviour. In case of a head-on situation where the own ship is the give-way vessel:

$$\begin{aligned}\mathbb{X}_{COLREG} \equiv \{(\boldsymbol{\eta}, \boldsymbol{\nu}) \in \mathbb{R}^6 \,:\, &\forall t \in [t_d, t_e]((b^r_{OS,TS}(t) < 0)\\ &\wedge (\exists t^*_1.\, |\psi(t^*_1) - \psi(t_d)| \geq \Delta\psi_{app})\\ &\wedge ((\exists t^*_2.\, |U_{OS}(t^*_2) - U_{OS}(t_d)| \geq \Delta U_{app})\\ &\vee (U_{OS}(t^*_2) = U_{OS}(t_d))))\}\end{aligned} \tag{18}$$

in case of a crossing situation where the own ship is the give-way vessel:

$$\begin{aligned}\mathbb{X}_{COLREG} \equiv \{(\boldsymbol{\eta}, \boldsymbol{\nu}) \in \mathbb{R}^6 \,:\, &\forall t \in [t_d, t_e]((BCR_{TS,OS}(t) < 0)\\ &\wedge (\exists t^*_1.\, |\psi(t^*_1) - \psi(t_d)| \geq \Delta\psi_{app})\\ &\wedge ((\exists t^*_2.\, |U_{OS}(t^*_2) - U_{OS}(t_d)| \geq \Delta U_{app})\\ &\vee (U_{OS}(t^*_2) = U_{OS}(t_d))))\}\end{aligned} \tag{19}$$

in case of an overtaking situation where the own ship is the give-way vessel:

$$\begin{aligned}\mathbb{X}_{COLREG} \equiv \{(\boldsymbol{\eta}, \boldsymbol{\nu}) \in \mathbb{R}^6 \,:\, &\forall t \in [t_d, t_e]((\exists t^*_1.\, |\psi(t^*_1) - \psi(t_d)| \geq \Delta\psi_{app})\\ &\wedge ((\exists t^*_2.\, |U_{OS}(t^*_2) - U_{OS}(t_d)| \geq \Delta U_{app})\\ &\vee (U_{OS}(t^*_2) = U_{OS}(t_d))))\}\end{aligned} \tag{20}$$

in case of any situation where the own ship is the stand-on vessel:

$$\mathbb{X}_{COLREG} \equiv \{(\boldsymbol{\eta}, \boldsymbol{\nu}) \in \mathbb{R}^6 \,:\, \forall t \in [t_d, t_e]\left(\psi(t) = \psi(t_d) \wedge U(t) = U(t_d)\right)\} \tag{21}$$

5. Dynamic COLREG meta-classification description

The aim of this section is to describe how DCMC works and why it is able to overcome the issue of Classification Instability that affects SCMC. As the example in Section 3 showed, the key phenomenon behind Classification Instability is the lack of memory of the previous states of the encounter scenario in SCMC. To overcome Classification Instability it is thus necessary that DCMC exhibits a memory effect similar to the physical phenomenon of hysteresis: once a scenario has been classified, DCMC should keep returning the same output even when the conditions that triggered that output are not in place anymore, then change the output only when very different conditions appear. This behaviour in COLREG classification is referred to as COLREG Hysteresis (Kuwata et al., 2014).

To achieve COLREG Hysteresis, DCMC makes use of four things: a CC system, a CRA methodology, a memory device, and a PACC. The CC system is used to classify a scenario when no previous information is available. The memory device is used to retain the information of the previous states of the encounter scenario together with the previous outputs of the CC system. The PACC is a rule that verifies whether the requirements from Rule 13 and Rule 8 from COLREG are satisfied. The aim of the PACC is to decide whether it is necessary to reclassify again the current state of the encounter scenario, thus triggering the CC system, or the previous classification result stored in the memory device should be used. To make DCMC achieve COLREG Hysteresis, the PACC must be stricter than the condition used by the CRA methodology of choice. The process of DCMC is described by Algorithm 1:

Algorithm 1 (*Dynamic COLREG Meta-Classification*).

Step 1: At each time instant t_i check if the pair $(\mathbf{x}_{OS}(t_{i-1}), \mathbf{x}_{TS}(t_{i-1}))$ is in memory.
Step 2: If $(\mathbf{x}_{OS}(t_{i-1}), \mathbf{x}_{TS}(t_{i-1}))$ is in memory, check the PACC, else go to Step 4.
Step 3: If PACC is not satisfied return the COLREG situation and behaviours associated with $(\mathbf{x}_{OS}(t_{i-1}), \mathbf{x}_{TS}(t_{i-1}))$ and exit, else remove $(\mathbf{x}_{OS}(t_{i-1}), \mathbf{x}_{TS}(t_{i-1}))$ from memory and go to Step 4.
Step 4: Check with the CRA methodology of choice whether a risk of collision is present or not. If it is, classify $(\mathbf{x}_{OS}(t_i), \mathbf{x}_{TS}(t_i))$ according to the CC system of choice, add the $(\mathbf{x}_{OS}(t_i), \mathbf{x}_{TS}(t_i))$ together with resulting COLREG situation and behaviours to memory and return them; else exit.

This paper proposes the PACC shown in Eq. (22):

$$TCPA_{OS,TS}(t) < TCPA_{threshold} \tag{22}$$

with $TCPA_{threshold} < 0$. This formulation of the PACC achieves a double effect. Because $TCPA_{threshold}$ is negative, Eq. (22) implies that reclassification is triggered only when the closest point of approach is past both vessels and, therefore, they are on diverging routes. $TCPA_{threshold}$ acts as an adaptive buffer distance between vessels: in scenarios where the relative velocity between vessels is high and, therefore, the outcome of a collision would be catastrophic, Eq. (22) requires a relatively high distance between the vessels before reclassification is triggered; in scenarios where the relative velocity between vessels is low and, therefore, the outcome of a collision would be less severe, Eq. (22) requires a relatively small distance before reclassification is triggered.

6. Methodology

To assess the impact of DCMC on COLREG-compliant CA, a scenario-based testing procedure is employed: multiple encounter scenarios are simulated and insights on the performance of DCMC are derived by means of a quantitative analysis based on relevant metrics.

All encounter scenarios replicate a high sea setting in which two vessels are required to perform both Path Following (PF) and CA activities, thus creating the conditions for Classification Instability to arise, as described in Section 3. Each encounter scenario is simulated twice: the first time embedding SCMC into the CA system, the second time embedding DCMC. A comparison between the simulations is made using proper metrics described in Section 6.4.

To allow the vessels to carry out both PF and CA activities, they are independently controlled by a GNC system described in Section 6.3. Moreover, to minimise the bias of this study, the simulated encounter scenarios are generated using a randomised approach similar to that described by Pedersen et al. (2023) and properly described in Section 6.1. The simulations are carried out under the following conditions:

- All scenarios take place in open water, with perfect visibility between vessels which are considered to be on sight of one another;
- All vessels are Power-Driven Vessels as defined by Part B of COLREG;
- The course-based approach is the CC system of choice;
- The CPA-TCPA method is the CRA methodology of choice.

6.1. Randomised two-vessel encounter scenario generation

The encounter scenarios used for the simulation campaign are generated following a randomised approach to minimise the bias of this study. The encounter scenario generation procedure adopted in this paper is based on that proposed by Pedersen et al. (2023) with the difference that the desired COLREG situation is imposed based on the course-based CC approach instead of the bearing-based approach. The generated encounter scenarios must satisfy the following criteria:

Table 2
Geometrical characteristics of the ship.

Quantity	Value
Length overall [m]	171.80
Maximum beam [m]	23.16
Design draft [m]	8.23
Design displacement [t]	19 004

- When not at risk of collision, the vessels involved are required to sail along a straight route;
- Both vessels must detect a risk of collision after a given amount of time Δt_{action};
- The vessels involved must end up in a collision situation after a given amount of time equal to $\Delta t_{action} + TCPA_{alert}$;

The encounter scenario generation procedure proceeds as follows. The encounter scenario begins at t_0, and the time when the collision happens is denoted as $t^* = t_0 + \Delta t_{action} + TCPA_{alert}$. For a collision to occur between the two vessels it is necessary that their positions at t^* satisfy the condition below:

$$\sqrt{(x_{OS}(t^*) - x_{TS}(t^*))^2 + (y_{OS}(t^*) - y_{TS}(t^*))^2} = 0 \tag{23}$$

Without losing generality, it is possible to select arbitrarily $x_{OS}(t_0)$, $y_{OS}(t_0)$, ψ_{OS}, and U_{OS}. To simplify the procedure $x_{OS}(t_0)$ and $y_{OS}(t_0)$ are taken as the origin of the $\{n\}$ reference frame, ψ_{OS} is set to the True North while U_{OS} is chosen randomly between a maximum and minimum value U_{min} and U_{max}. Thus, $x_{OS}(t^*)$ and $y_{OS}(t^*)$ can be calculated as:

$$\begin{cases} x_{OS}(t^*) = x_{OS}(t_0) + (t^* - t_0)U_{OS}\cos(\psi_{OS}) \\ y_{OS}(t^*) = y_{OS}(t_0) + (t^* - t_0)U_{OS}\sin(\psi_{OS}) \end{cases} \tag{24}$$

and, since from Eq. (23) follows that $(x_{TS}(t^*), y_{TS}(t^*)) \equiv (x_{OS}(t^*), y_{OS}(t^*))$, $x_{TS}(t^*)$ and $y_{TS}(t^*)$ are known too.

If a COLREG situation and a pair of COLREG behaviours for the two vessels are selected randomly, a value for $\Delta\psi_{OS,TS}$ can be determined by randomly choosing within the ranges described in Table 1. Then, the heading of the target ship is calculated as $\psi_{TS} = \psi_{OS} + \Delta\psi_{OS,TS}$.

U_{TS} can be selected randomly with the only constraint emerging only in case an overtaking situation is desired. Finally, $x_{TS}(t_0)$ and $y_{TS}(t_0)$ are calculated as follows:

$$\begin{cases} x_{TS}(t_0) = x_{TS}(t_0) + (t^* - t_0)U_{TS}\cos(\psi_{TS} + \pi) \\ y_{TS}(t_0) = y_{TS}(t_0) + (t^* - t_0)U_{TS}\sin(\psi_{TS} + \pi) \end{cases} \tag{25}$$

6.2. Dynamical models of the ships

For all ships in the simulations, the vessel model described in Chislett and Strom-Tejsen (1965) is adopted. This model is derived from planar motion mechanism tests on the model of a real ship belonging to the Mariner class of cargo vessels from the 1960s. The geometrical characteristics of the ship is shown in Table 2. The mathematical model is derived from the one in Eq. (26) where the functions f_X, f_Y, and f_N are approximated by third-order Taylor expansions:

$$\begin{cases} (m - X_{\dot{u}})\dot{u} & = f_X(u, v, r, \delta) \\ (m - Y_{\dot{v}})\dot{v} + (mx_G - Y\dot{r})\dot{r} & = f_Y(u, v, r, \delta) \\ (mx_G - N\dot{v})\dot{v} + (I_Z - N_{\dot{r}})\dot{r} & = f_N(u, v, r, \delta) \end{cases} \tag{26}$$

For the hydrodynamic coefficients, one should refer to the original publication.

6.3. Simulated GNC architecture

In the simulations, the vessels are controlled by a GNC system which is designed to guide the vessel model from Eq. (26) to satisfy two control objectives: follow a predetermined route and execute evasive

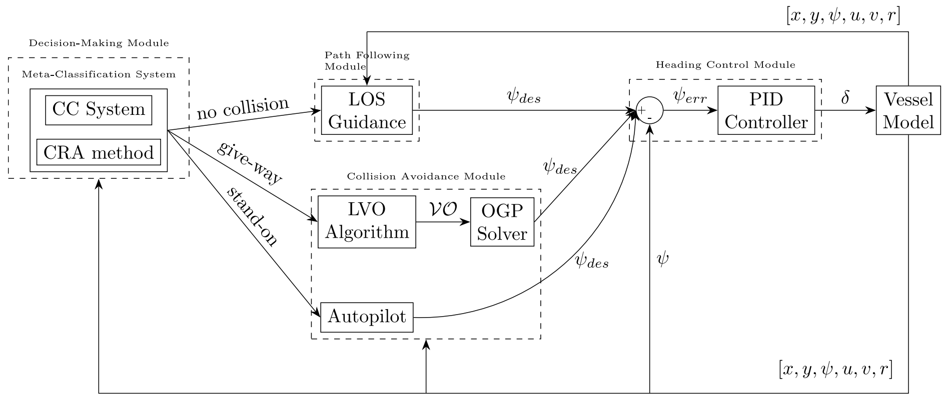

Fig. 4. Architecture of the GNC system employed in the simulations of the encounter scenarios.

manoeuvres. The first objective can be achieved by any path following algorithm suited for underactuated vessels, the second objective would require a control algorithm capable of solving the OCP from Eq. (17), which is a challenging task.

Since it is out of the scope of this paper to propose a novel GNC system for COLREG-compliant collision-free path following, a multiple guidance law system based on well-known algorithms drawn from literature is employed. In particular, the GNC system consists of four modules: the PF Module (PFM), the CA Module (CAM), the Decision-Making Module (DMM), and the Heading Control Module (HCM).

The PFM and the CAM represent two alternative guidance laws that can be used during the simulations: both produce a heading set point, denoted as ψ_{des}, but the first produces a value for ψ_{des} that ensures the convergence on the path, the second produces a value for ψ_{des} which solves the OCP from Eq. (17). The choice of which of these two guidance systems should compute ψ_{des} at each given instant is taken by the DMM. Finally, the HCM employs a Proportional, Integral, and Derivative (PID) controller to bring the own ship heading to ψ_{des}. A graphical schema of the architecture of the GNC system is provided in Fig. 4.

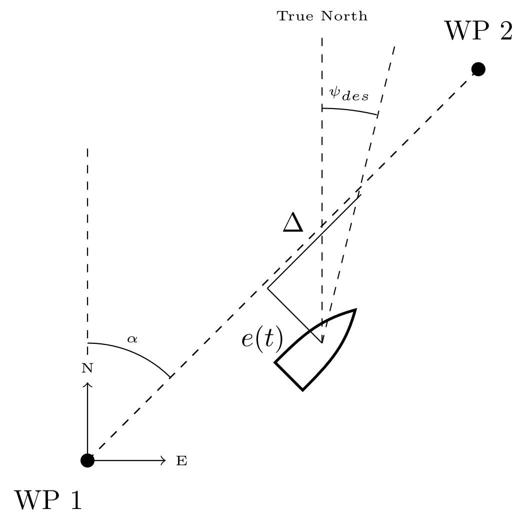

Fig. 5. Line Of Sight algorithm graphical summary.

6.3.1. *Lookahead-based Line Of Sight-based path following guidance*

To achieve its aim, the PFM implements a Line Of Sight (LOS) guidance algorithm. The reference implementation is described in Fossen (2011) as Lookahead-Based LOS. A graphical summary of the algorithm is shown in Fig. 5. At each time instant, the algorithm produces a ψ_{set} that makes the own ship move towards a point on the route that lies a certain distance Δ, called lookahead distance, from the position of the own ship projected on the route. This value of ψ_{set} is calculated as follows:

$$\psi_{set}(t) = \tan^{-1}\left(\frac{-e(t)}{\Delta}\right) \tag{27}$$

where $e(t)$ is the instantaneous cross-track error calculated as in Eq. (28):

$$e(t) = -(x_{OS}(t) - x_{WP_1})\cos(\alpha) + (y_{OS}(t) - y_{WP_1})\sin(\alpha) \tag{28}$$

where α is the route tangential angle with respect to the True North.

6.3.2. *Linear velocity obstacle-based collision avoidance guidance*

The aim of the CAM is to guide the MASS when a risk of collision is present. In such occasions the MASS is not necessarily required to execute an evasive manoeuvre; this depends on whether the MASS is the give-way vessel or the stand-on vessel in encounter scenario. The CAM must be able to guide the MASS in both cases. To do so, it embeds a Linear Velocity Obstacle (LVO)-based CA algorithm, to fulfil the give-way behaviour requirements, and a simple autopilot, to fulfil the stand-on behaviour requirements. The LVO-based CA algorithm is described in this section, the autopilot in Section 6.3.3

The LVO-based CA algorithm operates as follows. Firstly, an LVO algorithm is used to compute the set of all velocity vectors that lead to a collision with the target ship at a certain point in time. This set is denoted by $\mathcal{VO}$. The reference implementation for the LVO algorithm adopted in this paper comes from Huang et al. (2018). For a detailed description of the algorithm, one should refer to the original publication. Finally, an optimisation problem, referred to in this paper as an Optimal Guidance Problem (OGP), is then used to select among $\overline{\mathcal{VO}}$, i.e., the set of all collision-free velocity vectors, the one which satisfies COLREG requirements and minimises deviation from the planned route. The OGP is derived from the OCP from Eq. (17) by introducing some simplifying hypotheses.

Firstly, the dynamics of the own ship is neglected, thus, instead of looking for a control law $\mathbf{u}(t)$ which produces a collision-free velocity, it is possible to directly look for a collision-free velocity. Secondly, the constraints of Eq. (17) can be significantly simplified by neglecting the dynamics of the target ships and assuming they move on a straight line and at constant speed. Thirdly, the own ship is constrained to avoid collision using course change alone. This allows to rewrite the decision variable of the OGP as a heading ψ_{des} instead of a velocity vector, and it is also possible to rewrite the objective function as the difference

Table 3
Parameters of the CPA-TCPA method and PACC.

Parameter	Value
CPA_{alert}	1 nm
$TCPA_{alert}$	15 min
$TCPA_{threshold}$	−15 min

between ψ_{des} and ψ_{route}. The resulting OGP is shown in Eq. (29):

$$\begin{aligned}&\underset{\psi_{des}}{\operatorname{argmin}}(\psi_{des}-\psi_{route})^2\\ &\quad \text{s.t. C1: } \mathbf{v}^n_{OS}(t)\in\overline{\mathcal{VO}}\\ &\qquad \text{C2: } \psi_{des}\in\Psi\\ &\qquad \text{C3: } \begin{cases}\dot{x}_{OS}(t)=U_{OS}(t_0)\cos(\psi_{des})\\ \dot{y}_{OS}(t)=U_{OS}(t_0)\cos(\psi_{des})\end{cases}\\ &\qquad \text{C4: } \begin{cases}\dot{x}_{TS}(t)=U_{OS}(t_0)\cos(\psi_{TS}(t_0))\\ \dot{y}_{TS}(t)=U_{OS}(t_0)\cos(\psi_{TS}(t_0))\end{cases}\end{aligned} \tag{29}$$

where $\mathbf{v}^n_{OS}(t) = [\dot{x}_{OS}(t), \dot{y}_{OS}(t)]$ and Ψ is the feasibility set which represents the requirements of COLREG; in case of a crossing or head-on situation:

$$\Psi \equiv \{\psi\in\mathbb{R} : (\Delta\psi_{max}(t_0)\geq\Delta\psi_{APP})\wedge(b^r_{OS,TS}<0)\} \tag{30}$$

in case of an overtaking situation:

$$\Psi \equiv \{\psi\in\mathbb{R} : \Delta\psi_{max}(t_0)\geq\Delta\psi_{APP}\} \tag{31}$$

6.3.3. Autopilot

The autopilot simply returns the heading of the vessel when the collision risk was first detected. This guidance law is meant to satisfy the obligations of the stand-on behaviour.

6.3.4. COLREG classifier-based decision-making module

The DMM implements an algorithm that decides whether the own ship should be guided by the PFM or by the CAM and, in such a case, whether by the LVO-based CA or by the autopilot. To make this choice, the DMM makes use of a CC system and a Meta-Classification system. In particular, if the Meta-Classification system does not return a classification output, then ψ_{des} is calculated by the PFM; otherwise, if the own ship is recognised by the CC system as the stand-on vessel, then ψ_{des} is calculated by the autopilot while if the own ship is recognised as the give-way vessel, ψ_{des} is calculated by the LVO-based CA algorithm.

A stated in Section 6, the CPA-TCPA method is adopted as CRA methodology, the course-based approach is adopted as CC system, and, for the first round of simulations, DCMC is used, while for the second round of simulations, SCMC is used. The parameters of the CPA-TCPA method and for the PACC are shown in Table 3.

6.3.5. PID-based heading control module

The HCM computes the rudder angle required to achieve ψ_{des}. The control algorithm is a single-input single-output PID controller. The control law is shown in Eq. (32).

$$\delta(t) = K_P(\psi_{des}-\psi(t)) + K_I\int_0^t(\psi_{des}-\psi(\tau))\,d\tau + K_D\frac{d(\psi_{des}-\psi(t))}{dt} \tag{32}$$

6.4. Simulation metrics

Proper metrics are defined to interpret the results of the simulations. In particular, four metrics are defined: Classification Quality (CQ), to quantify the reliability of the classification output, distance at Closest Point of Approach (CPA), to quantify the safety of the evasive manoeuvre, Rule Compliance (RC), to quantify COLREG-compliance during the evasive manoeuvre, and Manoeuvre Unfeasibility (MU), to quantify and compare the difficulty of actuating the evasive manoeuvre.

6.4.1. Classification quality metric

The aim of the CQ metric is to assess the reliability of the classification output: the higher the numerical value of CQ, the more reliable the classifier output. To quantify this, this paper uses the mean over $[t_d, t_e]$ of a function $f_{C_0,C(t)}(t)$ defined as follows:

$$f_{C_0,C(t)}(t) = \begin{cases}1, & \text{if } C_0 = C(t)\\ 0, & \text{otherwise}\end{cases} \tag{33}$$

where C_0 is the expected classification output and $C(t)$ is the classification output obtained at time t. Using $f_{C_0,C(t)}(t)$, CQ is calculated as follows:

$$CQ = \frac{1}{t_e-t_d}\int_{t_d}^{t_e} f_{C_0,C(t)}(t)\,dt \tag{34}$$

6.4.2. Distance at closest point of approach metric

The CPA metric is identified as a relevant metric to compare collision avoidance algorithms (Zaccone et al., 2024). The CPA metric is defined as the minimum distance between the two agent ships in the time window $[t_d, t_e]$ normalised with respected to the safety distance d_{safety} introduced in Section 4.2.

$$CPA = \frac{\min(\{d_{AS_1,AS_2}(t) : t\in[t_d,t_e]\})}{d_{safety}} \tag{35}$$

6.4.3. Rule compliance metric

The RC metric aims to assess how much an evasive manoeuvre is compliant with the requirements from COLREG. To do so, proper functions called Compliance Functions, indicated with $C_S(t)$, are defined. These functions return at each time instant t a numerical value which quantifies how a certain vessel was in compliance with situation S at time instant t. The numerical value of each $C_S(t)$ ranges between 0 and 1, with 0 indicating complete violation and 1 full compliance. Once all the values of $C_S(t)$ in the range $[t_d, t_e]$ have been calculated, RC is calculated as follows:

$$RC = \frac{1}{t_e-t_d}\int_{t_d}^{t_e} C_S(t)\,dt \tag{36}$$

Five different Compliance Functions are defined, namely, $C_{HO}(t)$, $C_{CGW}(t)$, $C_{OGW}(t)$, $C_{CSO}(t)$, and $C_{OSO}(t)$, which quantify the compliance during a head-on, a crossing-give-way, an overtaking-give-way, a crossing-stand-on, and an overtaking-stand-on situation respectively. The complete definition of the Compliance Functions listed before can be found in the works of Woerner et al. (2019) and Gleeson et al. (2024). In this section, a brief description on the evaluation of these functions is shown.

The equations for the Compliance Functions are shown in Eq. (37)–(41):

$$C_{HO}(t) = (1-P_{DA}(t))(1-P_{NCC}(t))(1-P_{NSC}(t))(1-P_{PT}(t)) \tag{37}$$

$$C_{CGW}(t) = (1-P_{DA}(t))(1-P_{NCC}(t))(1-P_{NSC}(t))(1-P_{PT}(t)) \tag{38}$$

$$C_{OGW}(t) = (1-P_{DA}(t))(1-P_{NCC}(t))(1-P_{NSC}(t)) \tag{39}$$

$$C_{CSO}(t) = (1-P_{CC}(t))(1-P_{SC}(t)) \tag{40}$$

$$C_{OSO}(t) = (1-P_{CC}(t))(1-P_{SC}(t)) \tag{41}$$

where $P_{DA}(t)$, $P_{NC}(t)$, $P_{PT}(t)$, $P_{NSC}(t)$, $P_{CC}(t)$, and $P_{SC}(t)$ are Penalty Functions, i.e., functions quantifying a specific behaviour which reduces the compliance with the requirements of COLREG.

The penalty $P_{DA}(t)$ is calculated as in Eq. (42) and it penalises the delay of the evasive manoeuvre after the detection of the risk of collision:

$$P_{DA}(t) = R(t)\frac{d_{OS,TS}(t_d)-\min(d_{OS,TS}(t_d), d_{OS,TS}(t_m))}{d_{OS,TS}(t_d)} \tag{42}$$

where t_m is the time instant when the evasive manoeuvre starts, and $R(t)$ is a penalty reduction function defined as in Eq. (43):

$$R(t) = \min\left(\frac{(t-t_d)^2}{T_r^2}, 1\right) \tag{43}$$

where T_r is the reaction time of the own ship. The role of $R(t)$ is to reduce the value of a Penalty Function to account for the fact that vessels need a non-negligible amount of time to change their course. The value of t_m is taken as the first time instant at which the variation of course with respect to the course at t_d exceeds in absolute value a tolerance $\Delta\psi_{TOL}$. The variation of course is indicated as $\Delta\psi(t)$ and is calculated according to the equation:

$$\Delta\psi(t) = \psi(t) - \psi(t_d) \tag{44}$$

The penalty $P_{NCC}(t)$ is calculated as in Eq. (45) and penalises a non-apparent course change:

$$P_{NCC}(t) = \begin{cases} R(t)\frac{\Delta\psi_{app}-\Delta\psi_{max}(t)}{\Delta\psi_{app}}, & \Delta\psi_{max}(t) \le \Delta\psi_{app} \\ 0, & \text{otherwise} \end{cases} \tag{45}$$

where $\Delta\psi_{APP}$ is the value of an apparent course change, and $\Delta\psi_{max}(t)$ is the maximum value of $\Delta\psi(t)$ achieved until time t, calculated as in Eq. (46):

$$\Delta\psi_{max}(t) = \max(\{\Delta\psi(\tau) : \tau \in [t_d, t]\}) \tag{46}$$

The penalty $P_{PT}(t)$ is calculated as in Eq. (47) and penalises port side turns of give-way vessels:

$$P_{PT}(t) = \begin{cases} 0, & A(t) = 0 \\ \min\left(\frac{|\Delta\psi(t)|}{\Delta\psi_{TOL}}, 1\right), & \Delta\psi(t) < 0 \\ 0, & \text{otherwise} \end{cases} \tag{47}$$

where $A(t)$ is a switch function which checks whether the own ship and the target ship are on converging courses and is defined in Eq. (48):

$$A(t) = \begin{cases} 1, & TCPA_{OS,TS}(t) > 0 \\ 0, & \text{otherwise} \end{cases} \tag{48}$$

The penalty $P_{NSC}(t)$ is calculated as in Eq. (49) and penalises non-apparent changes of speed:

$$P_{NSC}(t) = \begin{cases} R(t)\frac{\Delta U_{app}-\Delta U_{max}(t)}{\Delta U_{app}}, & \Delta U_{max}(t) \le \Delta U_{app} \\ 0, & \text{otherwise} \end{cases} \tag{49}$$

where $\Delta U_{max}(t)$ is the maximum speed change achieved at time instant t, calculated as in Eq. (50):

$$\Delta U_{max}(t) = \max(\{\Delta U(\tau) : \tau \in [t_d, t]\}) \tag{50}$$

The penalty $P_{CC}(t)$ is calculated as in Eq. (51) and penalises changes in course angle:

$$P_{CC}(t) = \begin{cases} 0, & \Delta\psi(t) < \Delta\psi_{TOL} \\ \frac{\Delta\psi(t)-\Delta\psi_{TOL}}{\Delta\psi_{APP}-\Delta\psi_{TOL}}, & \Delta\psi(t) < \Delta\psi_{APP} \\ 1, & \text{otherwise} \end{cases} \tag{51}$$

The penalty $P_{SC}(t)$ is calculated as in Eq. (52) and penalises changes in speed:

$$P_{SC}(t) = \begin{cases} 0, & \Delta U(t) < \Delta U_{TOL} \\ \frac{\Delta U(t)-\Delta U_{TOL}}{\Delta U_{APP}-\Delta U_{TOL}}, & \Delta U(t) < \Delta U_{APP} \\ 1, & \text{otherwise} \end{cases} \tag{52}$$

where $\Delta U(t)$ is calculated as follows:

$$\Delta U(t) = U(t) - U(t_d) \tag{53}$$

The values of the other parameters of the compliance functions are listed in Table 4. The values for ΔU_{APP} and ΔU_{TOL} are not defined since the evasive manoeuvre was constrained to be executed with the use of the rudder alone.

Table 4
Parameters of the compliance functions.

Parameter	Value
T_r	200 s
$\Delta\psi_{app}$	20°
$\Delta\psi_{TOL}$	2°
ΔU_{app}	n/d Kn
ΔU_{TOL}	n/d Kn

6.4.4. Manoeuvre unfeasibility metric

The MU metric is a quantification of the difficulty of the vessel actuators to execute an evasive manoeuvre: the higher the value of the MU metric, the more difficult it is to execute the manoeuvre. To quantify this, this paper proposes the use of the root mean square of the time derivative of the rudder angle. In this way, sudden changes in the rudder angle or continuous alterations make the manoeuvre score as more unfeasible for a real rudder machine, while slow changes make the evasive manoeuvre score as more feasible. The MU metric is calculated as follows:

$$MU = \sqrt{\frac{1}{t_e - t_d}\int_{t_d}^{t_e} \dot{\delta}^2 \, dt} \tag{54}$$

6.5. Simulation environment

The simulation environment and the GNC system have been implemented with the Python programming language using the NumPy (Harris et al., 2020) linear algebra library and the SciPy (Virtanen et al., 2020) scientific computing library. The solver RK45 implemented in SciPy was used to numerically integrate the system in Eq. (26), and brute force was used to solve Eq. (29). The simulations were run on a laptop running Fedora Linux 40 (Workstation Edition) and equipped with an Intel Core i9-14900HX × 32 processor and 16 GB RAM.

7. Results of the simulation campaign

A pool of 100 scenarios was generated and used for the simulation campaign. In Fig. 6 the distribution of the COLREG situations in the scenario pool is shown. Since in the simulations both vessels were controlled independently by the GNC system described in Section 6.3, the usual terms own ship and target ship lose their meaning as there is no privileged point of view. Instead, the terms "agent ship 1" and "agent ship 2" are used to indicate the vessels involved in the scenarios. Moreover, the terms HO, CGW, CSO, OGW, OSO, and NC are used to indicate head-on situations, crossing situations where the agent ship 1 is the give-way vessel, crossing situations where the agent ship 1 is the stand-on vessel, overtaking situations where the agent ship 1 is the give-way vessel, overtaking situations where the agent ship 1 is the stand-on vessel, and situations where no risk of collision is detected respectively. Section 7.1 features some notable cases from the pool of simulated scenarios, while Section 7.2 shows the overall results of the simulation campaign by means of violin plots and tables.

7.1. Comparative analysis of notable scenarios

Figs. 7 to 12 show examples of head-on, crossing and overtaking situations using DCMC and SCMC from the pool of simulations carried out for this study. The differences between the simulations employing SCMC and those employing DCMC become evident by comparing Figs. 7(a), 9(a) and 11(a) with Figs. 8(a), 10(a) and 12(a), respectively, which show the trajectories of the evasive manoeuvres. While in Figs. 7(a), 9(a) and 11(a) the manoeuvres are smooth and last longer in time, in Figs. 8(a), 10(a) and 12(a) the manoeuvres are sharper and last less time.

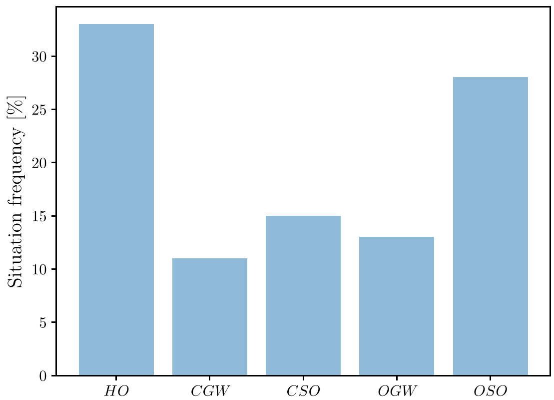

Fig. 6. Simulation dataset description.

Despite the differences, however, the evasive manoeuvres are executed correctly in all the simulations: the head-on and crossing situations feature a starboard turn, a wide initial course change, and in all of them the safety distance is respected, as show by Figs. 7(b), 8(b), 9(b), 10(b), 11(b) and 12(b). However, the consequences of Classification Instability become evident when examining Figs. 8(c), 8(d), 10(c), 10(d), 12(c) and 12(d).

Figs. 8(c), 10(c) and 12(c) show the time history of the rudder angle during the simulations employing SCMC. In all these figures, the rudder angle features an oscillatory behaviour in which the peaks of the oscillations come close to the maximum allowed value. Even though such rudder angles time histories can be actuated in a simulated environment, in a real world scenario they would cause excessive lateral accelerations that would harm crew, passengers and cargo and would cause fatigue to the rudder machine.

Figs. 8(d), 10(d) and 12(d) show the output of COLREG classification during the simulations employing SCMC. In all situations the classification results oscillate between the correct situation and NC rendering the CC system unreliable.

The same problems do not appear the simulations employing DCMC. In Figs. 7(c), 9(c) and 11(c) the rudder angle stays for most of the time on the steady state value, which is not zero since the vessel model is equipped with a single-screw propeller, and it changes only when the vessel is required to deviate from the predefined path and to return to it. In Figs. 7(d), 9(d) and 11(d) the output of the classifier remains stable on the correct value for the whole duration of the evasive manoeuvre, shifting back to NC only once, when the vessels are past and clear.

7.2. Overall results

Figs. 13(a) to 13(d) show by means of violin plots the distribution of the values of the relevant metrics defined in Section 6.4 over all the simulations carried out during this study.

Fig. 13(a) shows the distribution of the CQ metric with two violins: one for simulations carried out using the SCMC, the other for simulations carried out using DCMC. The plot for the simulations driven by the SCMC alone shows that the realised values of CQ are spread over all the domain of the metric and not even in one occasion its maximum value was reached. On the contrary, in all the simulations driven by DCMC the value of CQ is always at its maximum showing reliability and absence of Classification Instability.

Fig. 13(b) shows the distribution of the CPA metric with two violins: one for simulations carried out using the SCMC, the other for simulations carried out using DCMC. Both plots show a high concentration of values around or even above the value of 1 showing that independently of the Meta-Classification system used in no scenario the vessels ended up in a collision. However, in the simulations driven by DCMC, the CPA assumes higher values on average and d_{safety} is violated more rarely.

Table 5
Summary of results.

Metric	SCMC	DCMC	Improvement
μ_{CQ}	0.672	1	+48.77%
μ_{CPA}	0.996	1.001	+0.519%
μ_{RC}	0.965	0.984	+2.045%
$\mu_{MF_{SO}}$	$4.525 \cdot 10^{-4}$	$3.617 \cdot 10^{-6}$	−99.20%
$\mu_{MF_{GW}}$	$7.916 \cdot 10^{-3}$	$8.572 \cdot 10^{-4}$	−89.17%
Share of violations	86%	3%	−96.51%

Fig. 13(c) shows the distribution of the RC metric with two violins: one for simulations carried out using the SCMC, the other for simulations carried out using DCMC. This figure shows that RC is only slightly affected by the choice of Meta-Classification technique, instead, both SCMC and DCMC manage to reach high level of RC.

Fig. 13(d) shows the distribution of the MU metric with four violins: one for the stand-on vessel in simulations carried out using the SCMC (the violin named “SSO” in the figure), another for the stand-on vessel in simulations carried out using DCMC (the violin named “DSO” in the figure), another for the give-way vessel in simulations carried out using the SCMC (the violin named “SGW” in the figure), and the last one for the give-way vessel in simulations carried out using DCMC (the violin named “DGW” in the figure). This figure shows that the use of DCMC consistently reduces the unfeasibility of the manoeuvre both for the stand-on vessel and for the give-way vessel with compared to the SCMC.

Table 5 summarises the results already shown by Figs. 13(a) to 13(d) showing the mean values of the metrics and the variation in percentage of these quantities between the simulations that used the SCMC and those using DCMC. Moreover, the share of simulations where d_{safety} is violated is shown.

8. Conclusions

This work features a study of the phenomenon of Classification Instability which arises in the process of COLREG-compliant marine CA for MASS. The concept of Meta-Classification system is introduced to indicate those elements that link together the CC system and the CA algorithm in a GNC system for COLREG-compliant CA. Then the lack of memory of the previous states of the encounter scenario is identified as the source of Classification Instability in SCMC. DCMC is introduced as a replacement for SCMC as Meta-Classification system to solve the issue of Classification Instability. The performance of DCMC and SCMC are compared with the use of numerical simulations of two-vessel encounter scenarios. The results summarised in Table 5 show that DCMC is capable of solving the issue of Classification Instability and this fact is confirmed by the value of μ_{CQ} which is equal to 1.0 for the simulations in which DCMC is used. The simulation campaign shows that DCMC is also able to reduce the usage of the rudder during evasive manoeuvres making them more feasible for a real rudder machine. The number of scenarios where d_{safety} is violated is also lower in simulations where DCMC is used. The small variations in the values of μ_{CPA} and μ_{RC} between the simulations employing SCMC and those employing DCMC show that SCMC is still a valid Meta-Classification system, confirming its wide usage in the literature.

Further work can still be done in this direction. The simulations presented in this work could be carried out using different CC systems, CRA methodologies and CA algorithms. More COLREG situations could be simulated including different categories of vessels, e.g., sailing vessels, vessels engaged in fishing activities.

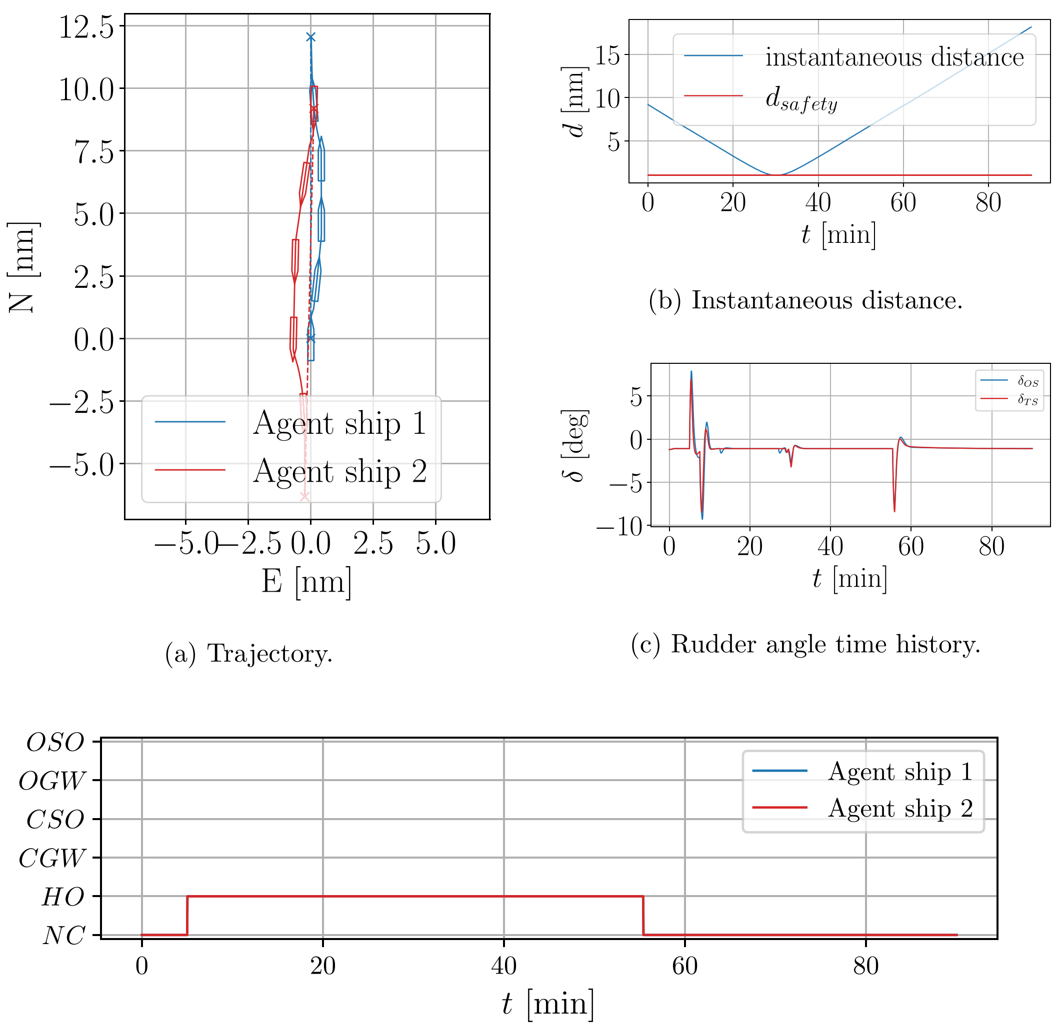

(a) Trajectory.

(b) Instantaneous distance.

(c) Rudder angle time history.

(d) Classification time history.

Fig. 7. Notable head-on scenario simulated with DCMC.

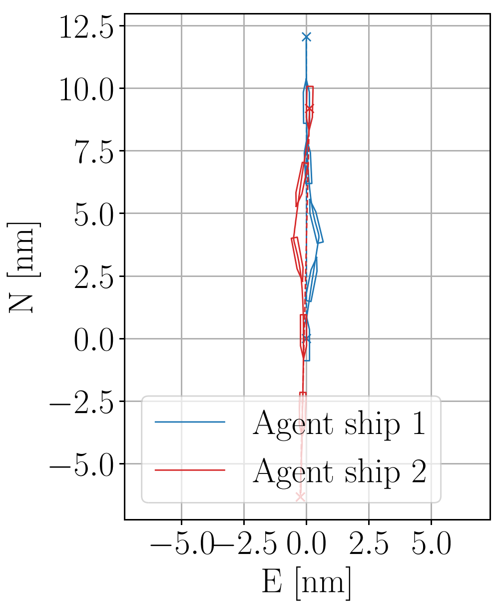

(a) Trajectory.

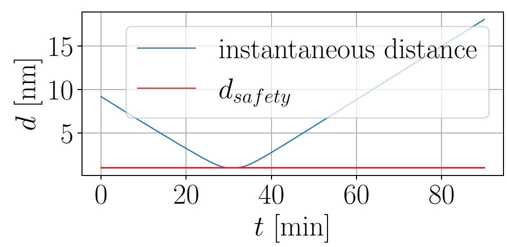

(b) Instantaneous distance.

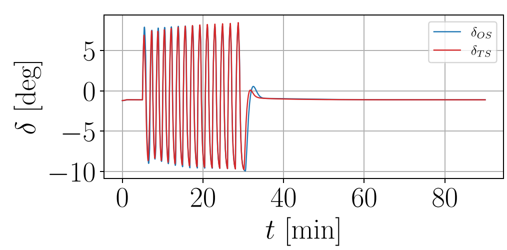

(c) Rudder angle time history.

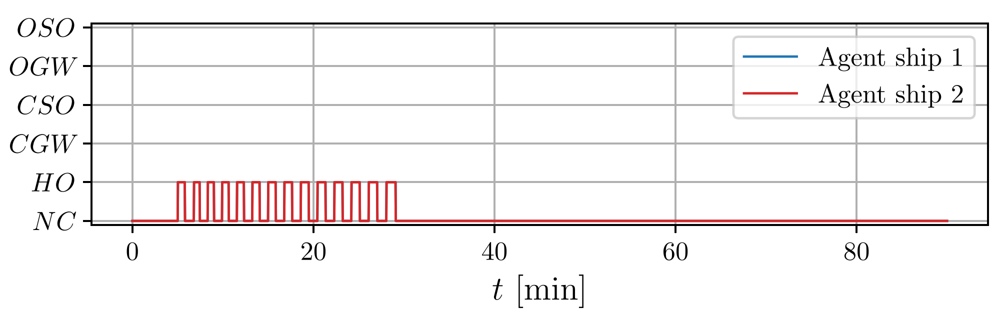

(d) Classification time history.

Fig. 8. Notable head-on scenario simulated with SCMC.

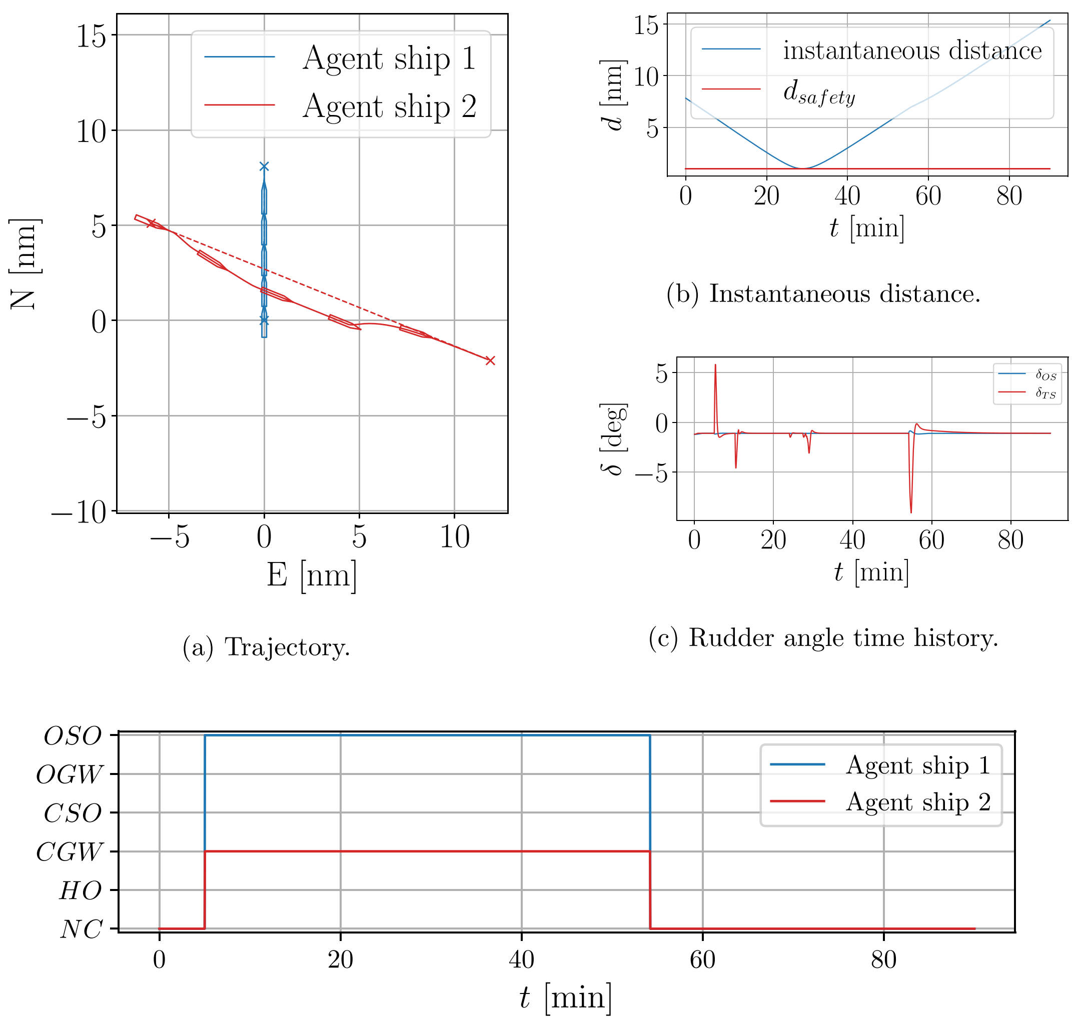

(a) Trajectory.

(b) Instantaneous distance.

(c) Rudder angle time history.

(d) Classification time history.

Fig. 9. Notable crossing scenario simulated with DCMC.

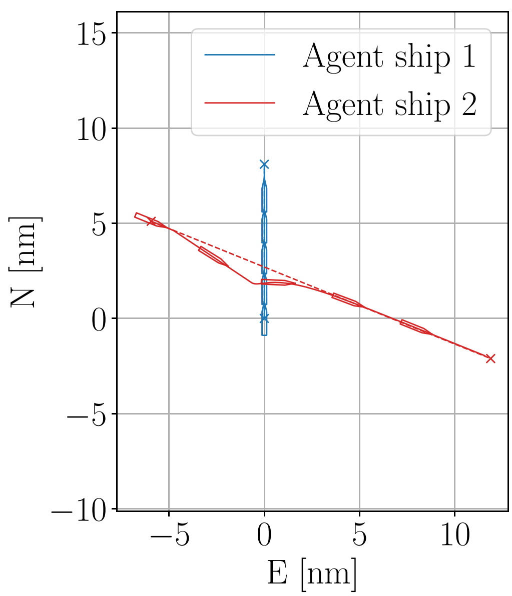

(a) Trajectory.

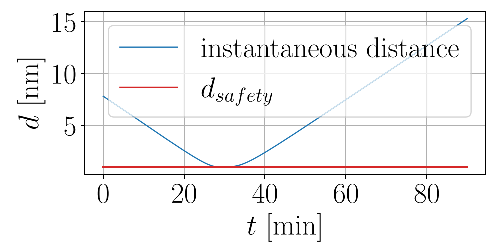

(b) Instantaneous distance.

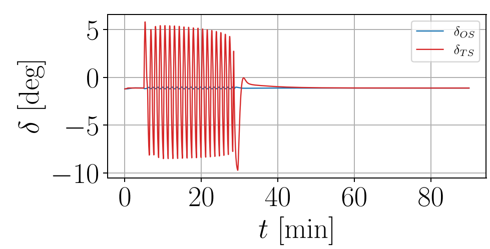

(c) Rudder angle time history.

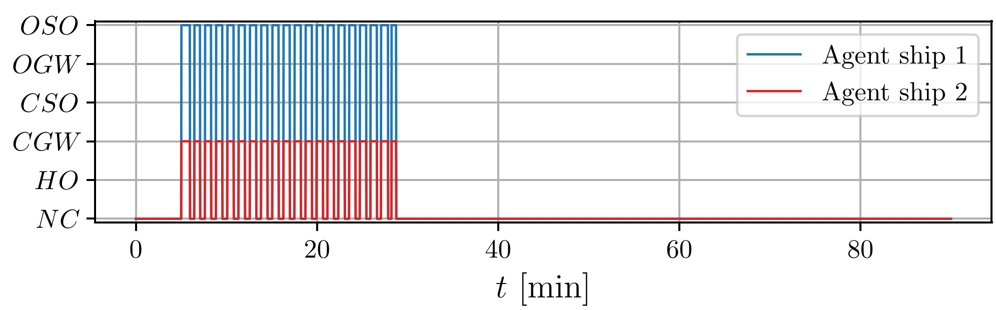

(d) Classification time history.

Fig. 10. Notable crossing scenario simulated with SCMC.

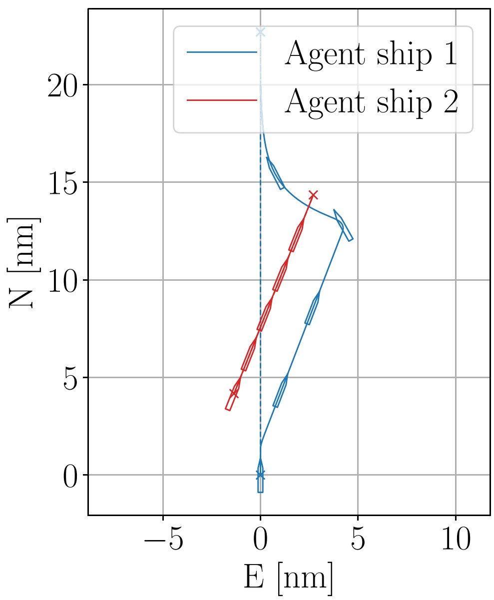

(a) Trajectory.

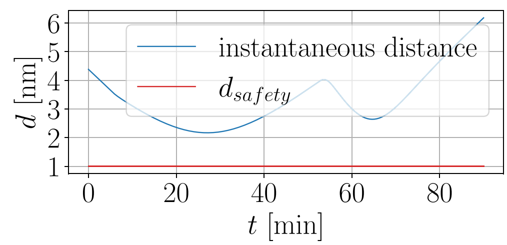

(b) Instantaneous distance.

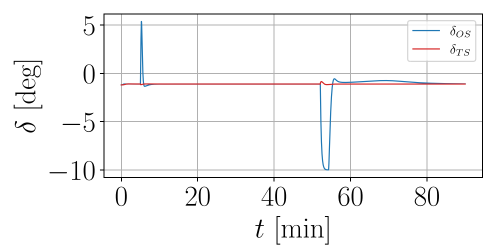

(c) Rudder angle time history.

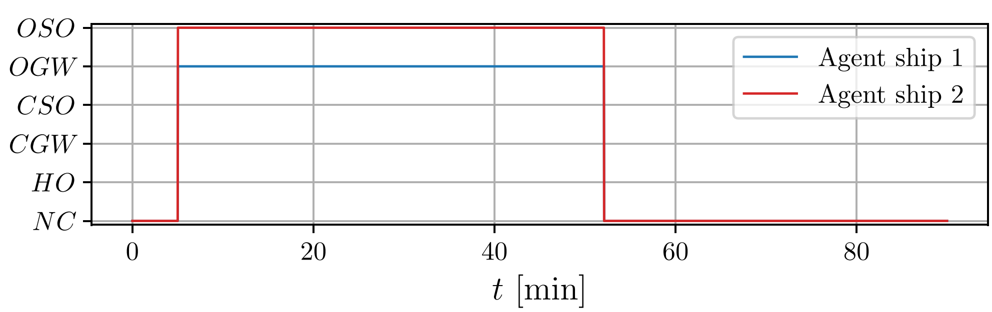

(d) Classification time history.

Fig. 11. Notable overtaking scenario simulated with DCMC.

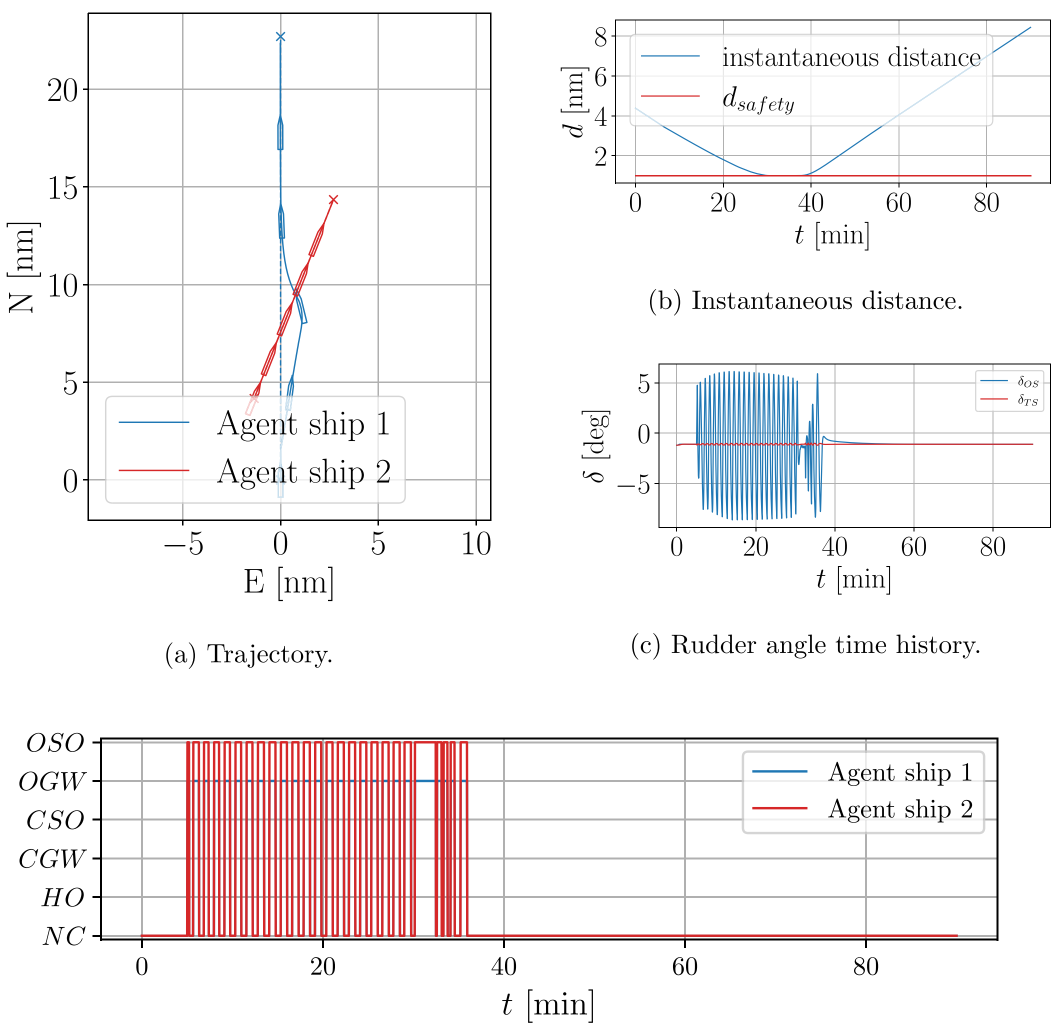

(a) Trajectory.

(b) Instantaneous distance.

(c) Rudder angle time history.

(d) Classification time history.

Fig. 12. Notable overtaking scenario simulated with SCMC.

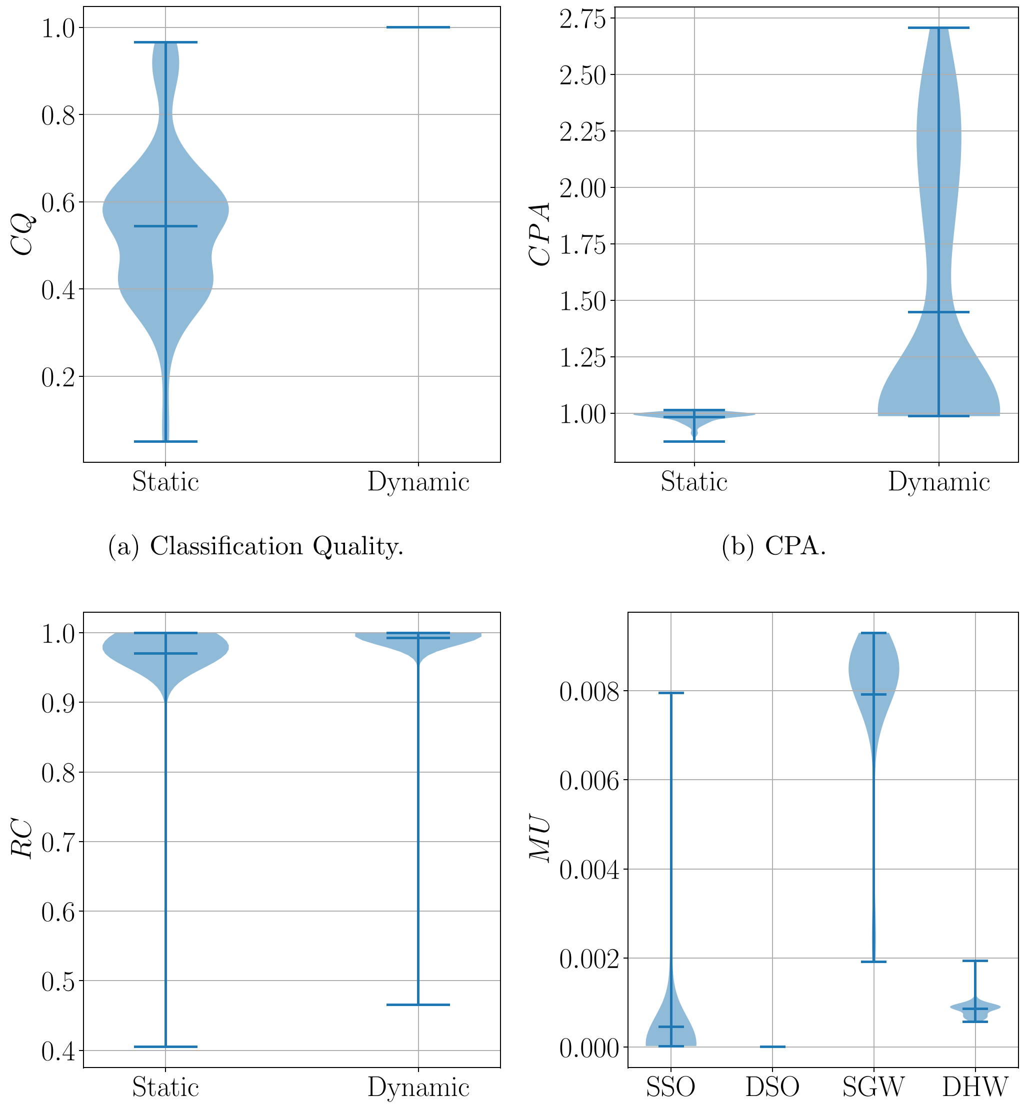

(a) Classification Quality. (b) CPA.

(c) Rule Compliance. (d) Manoeuvre Unfeasibility.

Fig. 13. Relevant metrics over all simulations.

CRediT authorship contribution statement

Nicola Sabatino: Writing – original draft, Visualization, Validation, Software, Methodology, Investigation, Formal analysis, Data curation, Conceptualization. **Raphael Zaccone:** Writing – review & editing, Validation, Supervision, Methodology, Conceptualization.

Declaration of competing interest

The authors declare that they have no known competing financial interests or personal relationships that could have appeared to influence the work reported in this paper.

References

Alamoush, A.S., Ölçer, A.I., F.B., 2024. Drivers, opportunities, and barriers, for adoption of maritime autonomous surface ships (mass). J. Int. Marit. Saf. Environ. Aff. Shipp. 8, 2411183. http://dx.doi.org/10.1080/25725084.2024.2411183.

Chislett, M., Strom-Tejsen, J., 1965. Planar motion mechanism tests and full-scale steering and manoeuvring predictions for a mariner class vessel. Int. Shipbuild. Prog. 12, 201–224.

Cho, Y., Han, J., Kim, J., 2022. Efficient colreg-compliant collision avoidance in multi-ship encounter situations. IEEE Trans. Intell. Transp. Syst. 23, 1899–1911. http://dx.doi.org/10.1109/TITS.2020.3029279.

EMSA, 2024. Annual overview of marine casualties and incidents 2024. URL: https://www.emsa.europa.eu/accident-investigation-publications/annual-overview.html. (Accessed 27 June 2025).

Enevoldsen, T.T., Reinartz, C., Galeazzi, R., 2021. Colregs-informed rrt* for collision avoidance of marine crafts. In: 2021 IEEE International Conference on Robotics and Automation. ICRA, IEEE, pp. 8083–8089.

Eriksen, B.O.H., Bitar, G., Breivik, M., Lekkas, A.M., 2020. Hybrid collision avoidance for asvs compliant with colregs rules 8 and 13–17. Front. Robot. AI 7 - 2020, http://dx.doi.org/10.3389/frobt.2020.00011, URL: https://www.frontiersin.org/journals/robotics-and-ai/articles/10.3389/frobt.2020.00011.

Fossen, T.I., 2011. Handbook of Marine Craft Hydrodynamics and Motion Control. John Wiley & Sons.

Fruzzetti, C., Ponzini, F., Sabatino, N., Donnarumma, S., Zaccone, R., Martelli, M., 2026. Field experiments on real-time autonomous marine surveillance. J. Mar. Eng. Technol. http://dx.doi.org/10.1080/20464177.2026.2648364, URL: https://www.scopus.com/inward/record.uri?eid=2-s2.0-105035145592&doi=10.1080%2f20464177.2026.2648364&partnerID=40&md5=715f5380de5b866e50f7a882b291fab4.

Fujii, Y., Tanaka, K., 1971. Traffic capacity. J. Navig. 24, 543–552. http://dx.doi.org/10.1017/S0373463300022384.

Gleeson, J., Dunbabin, M., Ford, J.J., 2024. Colreg scenario classification and compliance evaluation with temporal and multi-vessel awareness for collision avoidance systems. Ocean Eng. 313, 119552. http://dx.doi.org/10.1016/

j.oceaneng.2024.119552, URL: https://www.sciencedirect.com/science/article/pii/S0029801824028907.

Harris, C.R., Millman, K.J., van der Walt, S.J., Gommers, R., Virtanen, P., Cournapeau, D., Wieser, E., Taylor, J., Berg, S., Smith, N.J., Kern, R., Picus, M., Hoyer, S., van Kerkwijk, M.H., Brett, M., Haldane, A., del Río, J.F., Wiebe, M., Peterson, P., Gérard-Marchant, P., Sheppard, K., Reddy, T., Weckesser, W., Abbasi, H., Gohlke, C., Oliphant, T.E., 2020. Array programming with NumPy. Nature 585, 357–362. http://dx.doi.org/10.1038/s41586-020-2649-2.

Hasegawa, K., 1987. Automatic collision avoidance system for ships using fuzzy control. In: 8th Ship Control System Symposium. Hague.

Huang, Y., Chen, L., Chen, P., Negenborn, R.R., van Gelder, P., 2020. Ship collision avoidance methods: State-of-the-art. Saf. Sci. 121, 451–473. http://dx.doi.org/10.1016/j.ssci.2019.09.018, URL: https://www.sciencedirect.com/science/article/pii/S0925753519306356.

Huang, Y., van Gelder, P., Wen, Y., 2018. Velocity obstacle algorithms for collision prevention at sea. Ocean Eng. 151, 308–321. http://dx.doi.org/10.1016/j.oceaneng.2018.01.001, URL: https://www.sciencedirect.com/science/article/pii/S0029801818300015.

IMO, 2021. Outcome of the regulatory scoping exercise for the use of maritime autonomous surface ships (mass). URL: https://wwwcdn.imo.org/localresources/en/MediaCentre/HotTopics/PublishingImages/Pages/Autonomous-shipping/MSC.1-Circ.1638%20-%20Outcome%20Of%20The%20Regulatory%20Scoping%20ExerciseFor%20The%20Use%20Of%20Maritime%20Autonomous%20Surface%20Ships...%20(Secretariat).pdf. (Accessed 30 June 2025).

Kang, Y.T., Chen, W.J., Zhu, D.Q., Wang, J.H., Xie, Q.M., 2018. Collision avoidance path planning for ships by particle swarm optimization. J. Mar. Sci. Technol. 26, 3.

Kijima, K., Furukawa, Y., 2003. Automatic collision avoidance system using the concept of blocking area. IFAC Proc. Vol. 36, 223–228. http://dx.doi.org/10.1016/S1474-6670(17)37811-4, URL: https://www.sciencedirect.com/science/article/pii/S1474667017378114. 6th IFAC Conference on Manoeuvring and Control of Marine Craft (MCMC 2003), Girona, Spain, 17-19 September, 1997.

Kuwata, Y., Wolf, M.T., Zarzhitsky, D., Huntsberger, T.L., 2014. Safe maritime autonomous navigation with colregs, using velocity obstacles. IEEE J. Ocean. Eng. 39, 110–119. http://dx.doi.org/10.1109/JOE.2013.2254214.

Lazarowska, A., 2015. Ship's trajectory planning for collision avoidance at sea based on ant colony optimisation. J. Navig. 68, 291–307. http://dx.doi.org/10.1017/S0373463314000708.

Lyu, H., Yin, Y., 2017. Ship's trajectory planning for collision avoidance at sea based on modified artificial potential field. In: 2017 2nd International Conference on Robotics and Automation Engineering. ICRAE, pp. 351–357. http://dx.doi.org/10.1109/ICRAE.2017.8291409.

Martelli, M., Žuškin, S., Cellerino, E., Zaccone, R., 2024. Ship collision detection and classification employing ais data. All Days, ISOPE–I–24–474.

Meyer, E., Heiberg, A., Rasheed, A., San, O., 2020. Colreg-compliant collision avoidance for unmanned surface vehicle using deep reinforcement learning. IEEE Access 8, 165344–165364. http://dx.doi.org/10.1109/ACCESS.2020.3022600.

Namgung, H., Kim, J.S., 2021. Collision risk inference system for maritime autonomous surface ships using colregs rules compliant collision avoidance. IEEE Access 9, 7823–7835. http://dx.doi.org/10.1109/ACCESS.2021.3049238.

Pedersen, T.A., Vasanthan, C., Karolius, K., Engelhardtsen, Ø., Houweling, K.P., Jørgensen, A., 2023. Generating structured set of encounters for verifying automated collision and grounding avoidance systems. J. Phys.: Conf. Ser. 2618, 012013. http://dx.doi.org/10.1088/1742-6596/2618/1/012013.

Seo, C., Noh, Y., Abebe, M., Kang, Y.J., Park, S., Kwon, C., 2023. Ship collision avoidance route planning using CRI-based A* algorithm. Int. J. Nav. Archit. Ocean. Eng. 15, 100551.

Singh, Y., Sharma, S., Sutton, R., Hatton, D., 2017. Optimal path planning of an unmanned surface vehicle in a real-time marine environment using a Dijkstra algorithm. In: Marine Navigation. CRC Press, pp. 399–402.

Tam, C., Bucknall, R., 2010. Collision risk assessment for ships. J. Mar. Sci. Technol. 15, 257–270. http://dx.doi.org/10.1007/s00773-010-0089-7.

Virtanen, P., Gommers, R., Oliphant, T.E., Haberland, M., Reddy, T., Cournapeau, D., Burovski, E., Peterson, P., Weckesser, W., Bright, J., van der Walt, S.J., Brett, M., Wilson, J., Millman, K.J., Mayorov, N., Nelson, A.R.J., Jones, E., Kern, R., Larson, E., Carey, C.J., Polat, İ., Feng, Y., Moore, E.W., VanderPlas, J., Laxalde, D., Perktold, J., Cimrman, R., Henriksen, I., Quintero, E.A., Harris, C.R., Archibald, A.M., Ribeiro, A.H., Pedregosa, F., van Mulbregt, P., SciPy 1.0 Contributors, 2020. SciPy 1.0: Fundamental algorithms for scientific computing in Python. Nature Methods 17, 261–272. http://dx.doi.org/10.1038/s41592-019-0686-2.

Wang, Z., Chen, P., Mou, J., Chen, L., 2023. Colregs-compliant autonomous collision avoidance method based on deep reinforcement learning for usvs. In: 2023 7th International Conference on Transportation Information and Safety. ICTIS, pp. 1575–1598. http://dx.doi.org/10.1109/ICTIS60134.2023.10243729.

Wang, D., Wang, P., Zhang, X., Guo, X., Shu, Y., Tian, X., 2020. An obstacle avoidance strategy for the wave glider based on the improved artificial potential field and collision prediction model. Ocean Eng. 206, 107356. http://dx.doi.org/10.1016/j.oceaneng.2020.107356, URL: https://www.sciencedirect.com/science/article/pii/S0029801820303875.

Woerner, K., Benjamin, M.R., Novitzky, M., Leonard, J.J., 2019. Quantifying protocol evaluation for autonomous collision avoidance. Auton. Robots 43, 967–991. http://dx.doi.org/10.1007/s10514-018-9765-y.

Zaccone, R., 2024. A dynamic programming approach to the collision avoidance of autonomous ships. Mathematics 12, 1546.

Zaccone, R., Donnarumma, S., Martelli, M., 2024. A structured metric approach to compare marine collision avoidance algorithms. In: Conference Proceedings of ISCSS.

Zaccone, R., Martelli, M., 2020. A collision avoidance algorithm for ship guidance applications. J. Mar. Eng. Technol. 19, 62–75. http://dx.doi.org/10.1080/20464177.2019.1685836.

Zaccone, R., Martelli, M., Figari, M., 2019. A colreg-compliant ship collision avoidance algorithm. In: 2019 18th European Control Conference. ECC, pp. 2530–2535. http://dx.doi.org/10.23919/ECC.2019.8796207.

Zaccone, R., Ponzini, F., Martelli, M., 2026. Experimental validation of a modular navigation architecture for marine autonomous surface vehicles with reactive collision avoidance. Appl. Ocean Res. 166, http://dx.doi.org/10.1016/j.apor.2025.104903, URL: https://www.scopus.com/inward/record.uri?eid=2-s2.0-105026997695&doi=10.1016%2fj.apor.2025.104903&partnerID=40&md5=e62d46b8c97077df36cce42653d89f93.